Letter

Logarithmic expansion of many-body wave packets in random potentials

Arindam Mallick* and Sergej Flach†
Center for Theoretical Physics of Complex Systems, Institute for Basic Science (IBS), Daejeon 34126, Korea

(Received 13 May 2021; accepted 3 February 2022; published 23 February 2022)

Anderson localization confines the wave function of a quantum particle in a one-dimensional random potential to a volume of the order of the localization length ξ. Nonlinear add-ons to the wave dynamics mimic many-body interactions on a mean-field level, and result in escape from the Anderson cage and in unlimited subdiffusion of the interacting cloud. We address quantum corrections to that subdiffusion by (i) using the ultrafast unitary Floquet dynamics of discrete-time quantum walks, (ii) an interaction strength ramping to speed up the subdiffusion, and (iii) an action discretization of the nonlinear terms. We observe the saturation of the cloud expansion of N particles to a volume $\sim N\xi$. We predict and observe a universal intermediate logarithmic expansion regime which connects the mean-field diffusion with the final saturation regime and is entirely controlled by particle number N. The temporal window of that regime grows exponentially with the localization length ξ.

DOI: 10.1103/PhysRevA.105.L020202

Introduction. Single-particle quantum dynamics in a one-dimensional space with uncorrelated disorder results in Anderson localization (AL), i.e., confinement to a finite localization volume of the order of the localization length ξ [1]. The evolution of an initially localized quantum wave packet will consist of an (almost ballistic) expansion up to the volume $\sim\xi$ [2] with a subsequent halt and exponential wave-function localization in the tails [3]. Experimental verifications of AL with Bose-Einstein condensates of ultracold atomic gases loaded onto optical potentials were reported harvesting on the halt of the wave-packet expansion [4].

Many-body interactions alter the picture. Full-scale computations of temporal evolutions are restricted to two or three interacting particles only, with the complexity quickly increasing due to the Hilbert space dimension proliferation [5–23]. Increasing the number of particles is predicted to result in a slow subdiffusive expansion [24], which adds to the computational challenge. The same slow subdiffusion limits experimental studies with condensates due to finite coherence times [25]. Treating infinite particle numbers with mean-field approximations results in nonlinear add-ons to the wave dynamics which stem from the two-body interactions. Nonlinear wave-packet expansion was investigated both analytically and numerically over vast timescales [26–32]. It allows us to obtain the details of the subdiffusion process, with expansion times which are many orders of magnitude larger than the time reached by the experimental implementations of comparable theoretical models [33]. Remarkably, the subdiffusive expansion of a nonlinear wave packet appears to show no signatures of halt which was tested using a vast number of different Hamiltonian and discrete-time map evolutions with various types of nonlinear terms [33]. Contrarily, for quantum clouds with N particles we expect the expansion to stop when the cloud reaches the size of the order of $N\xi$ since each particle can occupy its own localization volume $\sim\xi$ and is only exponentially weakly interacting with other particles.

Here, we want to explore the long-time wave-packet expansion of an interacting many-body cloud and to establish its slowing down from (sub)diffusion to a complete halt. To achieve that challenging goal, we have to choose proper platforms and approximations. We use a Floquet platform of discrete-time quantum walks which exhibit AL [34]. Nonlinear add-ons show subdiffusive cloud expansion up to record large evolution times [35]. We further use a time-dependent ramping of the interaction strength which allows us to speed up subdiffusion to normal diffusion [36]. Finally we quantize the actions in the nonlinear add-ons similar to the Bohr-Sommerfeld quantization approach and to previous quantization studies of kicked rotor models [37–40]. As a result, we are able to simulate the cloud expansion for tens and hundreds of interacting particles. We carefully choose the localization length ξ and the number of interacting particles in order to observe the slowing down and halt processes within the time window accessible due to computational restrictions. We succeed in observing a slowing down of the expansion into a universal intermediate logarithmic growth regime which connects the (sub)diffusion with the final saturation regime. We derive the analytical details of this logarithmic regime.

DTQW. The single-particle linear discrete-time quantum walk (DTQW) is a Floquet evolution of a two-level system $\{\sigma,\bar{\sigma}\}$ on a chain. The system state at time $t+1$ follows from that at time t by the following unitary map,

$$\psi_{n,\sigma}(t+1) = \cos\theta\,\psi_{n-1,\sigma}(t) + e^{i\phi_{n-1}(t)}\sin\theta\,\psi_{n-1,\bar{\sigma}}(t),$$
$$\psi_{n,\bar{\sigma}}(t+1) = -e^{-i\phi_{n+1}(t)}\sin\theta\,\psi_{n+1,\sigma}(t) + \cos\theta\,\psi_{n+1,\bar{\sigma}}(t), \quad (1)$$

where n counts the lattice sites, and θ is the mixing angle in the $\{\sigma,\bar{\sigma}\}$ space which controls the kinetic energy of an excitation [34]. The uncorrelated random on-site disorder in

*marindam@ibs.re.kr
†sflach@ibs.re.kr

the phase $\phi_n \equiv \zeta_n \in [-\pi, \pi]$ results in Anderson localization with the localization length $\xi = -[\ln(|\cos\theta|)]^{-1}$ [34]. Note that $\xi(\theta \to 0) \to \infty$ and $\xi(\theta \to \pi/2) \to 0$. DTQWs were introduced as a quantum version of classical random walks [41]. They serve as a single-particle version of a quantum cellular automaton [42,43]. DTQWs became a useful tool to study various systems and phenomena such as relativistic particles, artificial gauge fields [44,45], various topological phases [46–48], percolation problems [49,50], localization phenomena [51], and implementation of quantum information tasks [52–54], among others. DTQWs were implemented experimentally using NMR devices [55], optical devices [56,57], in the IBM quantum computer [58], and in a trapped ion quantum computer [59].

Nonlinearity was introduced in DTQWs in a number of publications [35,60–64]. We follow Ref. [35] by making the phase $\phi_n(t)$ a continuous function of the local norm $\rho_n(t) = |\psi_{n,\sigma}(t)|^2 + |\psi_{n,\bar{\sigma}}(t)|^2$:

$$\phi_n = \gamma \rho_n + \zeta_n. \tag{2}$$

Both linear and nonlinear DTQWs preserve the total norm $\mathcal{A} = \sum_n \rho_n$. We will evolve the DTQWs starting with one and the same localized initial condition $[\psi_{n,\sigma}(0), \psi_{n,\bar{\sigma}}(0)] = \delta_{n,0}[1, i]/\sqrt{2}$ with $\mathcal{A} = 1$. For $\gamma = 0$ the corresponding linear DTQW results in a short expansion and final halt of the wave packet spreading due to Anderson localization. Instead, for $\gamma \neq 0$ the wave packet continues its expansion beyond the limits set by Anderson localization [35]. Its root mean square (rms)

$$r = \sqrt{\langle n^2 \rangle - \langle n \rangle^2}, \quad \langle n^x \rangle = \sum_n n^x \rho_n, \tag{3}$$

grows indefinitely in a subdiffusive manner $r(t) \sim t^{1/6}$ [35].

Ramping. The subdiffusive expansion is a rather slow process since it is characterized by a time-dependent diffusion constant which is a function of the wave-packet norm density $\rho \sim 1/r$: $D \equiv D(\gamma\rho)$ [65]. The density ρ is decaying in time while the wave packet expands, thus effectively slowing down the diffusion. Since we intend to simulate the impact of a yet to be introduced quantum slowing down correction, we are facing a challenging computational task. Remarkably, there is a reported way to speed up the subdiffusive process by choosing a proper ramping of the strength of nonlinear interaction $\gamma(t)$. Such a ramping intends to compensate for the decrease of the density ρ through a proper increase of the interaction strength γ. That ramping can be in principle realized in experiments with ultracold atoms through a time-dependent magnetic field which controls the two-body scattering length in a vicinity to Feshbach resonances [66–69]. The ramping speedup scheme was successfully tested with a discrete nonlinear Schrödinger lattice Hamiltonian and a nonlinear quantum kicked rotor map [36]. We follow the ramping protocol from Ref. [36] and choose $\gamma(t) = \gamma t^\nu$:

$$\phi_n(t) = \gamma t^\nu \rho_n(t) + \zeta_n. \tag{4}$$

In a one-dimensional diffusive process for an initially localized wave packet, its variance grows linearly in time: $r^2 = Dt$. For the ramping case normal diffusion is reached when D is constant (stationary), implying that the product $(\gamma t^\nu \rho)$ inside the wave packet stays approximately constant. Since $\rho \sim 1/r$ and $r \sim \sqrt{t}$ for normal diffusion, we conclude that the ramping exponent $\nu = 1/2$ ensures normal diffusion of the wave packet (see also Ref. [36]). A further increase of the ramping exponent beyond $1/2$ does not modify the obtained normal diffusion [65]. Smaller ramping exponents gradually slow down the spreading into subdiffusion. Our numerical results in Fig. 1 confirm the above considerations. For what follows we will use $\nu = 1$ and $\gamma = 30$.

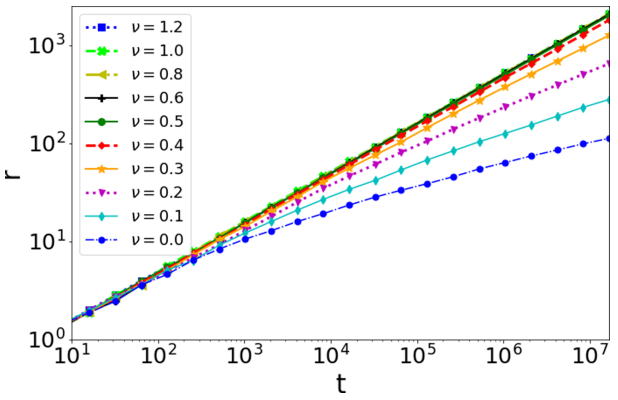

FIG. 1. Average of $\log r$ vs $\log t$ for expanding wave packets with ramping nonlinearity. The ramping exponent $\nu = 0, 0.1, 0.2, 0.3, 0.4, 0.5, 0.6, 0.8, 1.0, 1.2$ increases from bottom to top. Here, $\theta = 0.35\pi$ and $\gamma = 30$. Averaging is performed over 24 random disorder realizations.

Mimicking quantization through discretization. We arrived at the final and central part of our complex evolution design which intends to mimic a finite number of interacting quantum particles. The quantum analog of the total norm $\mathcal{A}$ is the number of particles N similar to the relation between the total norm of a Gross-Pitaevskii equation and the number of particles in a corresponding Bose-Hubbard Hamiltonian [70,71]. The quantum analog of the norm density ρ_n is the number of particles on that site. In analogy to the particle-number-dependent interaction energy of a many-body quantum lattice model we discretize the density ρ_n inside the nonlinear term [(2) and (4)] using a step function to arrive at

$$\phi_n(t) = \frac{\gamma t^\nu}{N} \lfloor N\rho_n(t) \rfloor + \zeta_n, \tag{5}$$

where $\lfloor N\rho_n(t) \rfloor$ is the largest possible integer less than or equal to $N\rho_n(t)$. The parameter $N \geqslant 1$ serves as the analog of the number of particles in a quantum many-body system. Note that the total number of particles $\sum_n N\rho_n(t) = N$ is conserved. For $N \to \infty$ we recover the continuous density dependence of the phase (4).

Figure 2(b) shows the computed dependence $\log r$ vs $\log t$ for $N = 24$, $\gamma = 30$, and $\nu = 1$ and a variety of different angles θ which control the single-particle localization length $\xi = -[\ln(|\cos\theta|)]^{-1}$. The wave packet initially expands diffusively and shows clear signatures of saturation and halt at larger evolution times. The rms value r at saturation can be expected to be of the order of the number of particles N times the volume of a one-particle Anderson localized wave packet v_l. That single-particle volume will depend on the localization length ξ and we will assess these details further below.

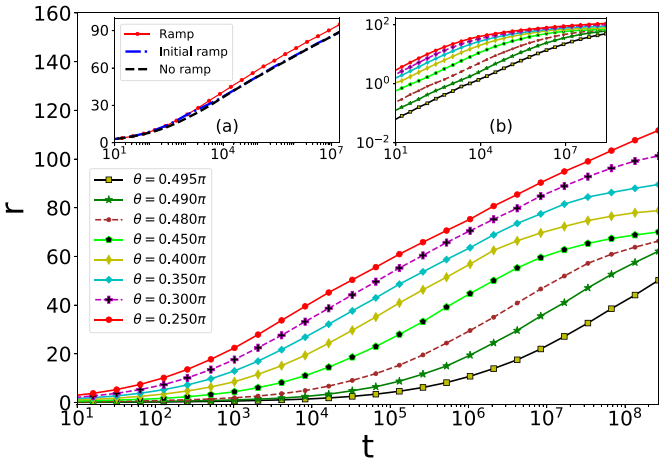

FIG. 2. Average of r vs $\log t$ for various values of θ (numbers in the legend, increasing from top to bottom) and $N = 24$. The average is taken over 177 random realizations. Inset (a) left: Average of r vs $\log t$ for $\theta = 0.25\pi$ and with ramping, only initial ramping, and no ramping (see text for details). Inset (b) right: The same main plot but in log-log scale. Averages are now taken for $\log r$.

Interestingly, Fig. 2(b) appears to predict that the saturation and halt will happen at earlier times the smaller the angle θ and therefore the larger the localization length ξ. However, a replot of the same data with r on a linear scale in the main part of Fig. 2 shows that what appeared to be a saturation and halt on logarithmic rms scales, turns into a *logarithmic expansion regime* of the quantized wave packet,

$$r(t) = r_0 + D_{\rm qn} \log_{10}(t), \tag{6}$$

where r_0 is a fitting parameter which will be quantified below. It can easily take negative values. The smaller θ and the larger ξ, the earlier the logarithmic expansion sets in, and the further it extends in time. In Fig. 2(a) we replot the data for $\theta = 0.25\pi$ and compare with a run where ramping is switched off when the rms reaches the value $r = 25$ where the logarithmic spreading regime appears to start. We also plot data from a run where no ramping is applied altogether. We observe very good agreement between all curves, which clearly shows that the ramping protocol is not affecting the essential details of the logarithmic spreading. The ramping though is crucial for larger θ values in order to faster reach the onset of logarithmic spreading.

To further substantiate this finding, we compute the local derivatives of the curves from the main panel of Fig. 2 and plot them in Fig. 3. We find that the derivatives show a plateau-like structure in the regime of logarithmic expansion, with a slope value $D_{\rm qn} \approx 20$, almost independently of θ and ξ. Logarithmic numerical derivatives are notorious for their fluctuations due to finite numbers of disorder realizations and smoothening operations resulting in slow fluctuations, therefore we will not analyze possible fine structures. Let us measure the true saturation time T_f. For that we find the largest slope position and value in Fig. 3. We then use the linear fit (6) and extend it to larger times until the rms reaches the assumed final localization volume $V_{\rm loc}$. The read-off time is identified as T_f:

$$T_f = 10^{(V_{\rm loc} - r_0)/D_{\rm qn}}. \tag{7}$$

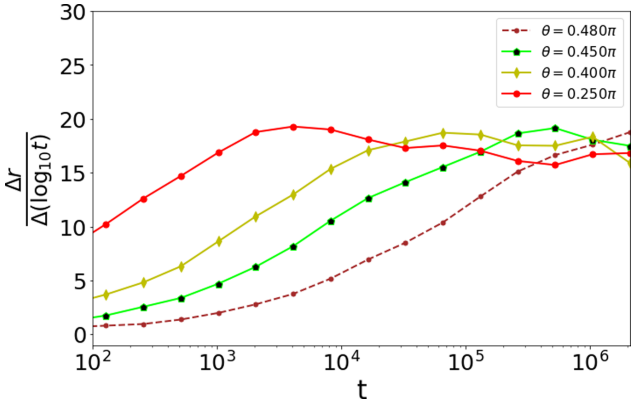

FIG. 3. Derivative of selected curves in Fig. 2 vs $\log t$. Only four θ values are shown for the sake of clarity. Curves for other θ values show similar behavior.

To estimate $V_{\rm loc}$ we assume that it is proportional to the number of particles N and the single-particle localization volume $v_l \approx r_l + 1$ where $r_l \sim \xi$ is the saturated rms of a single particle:

$$V_{\rm loc} = N f (r_l + 1). \tag{8}$$

Note that the correction by one integer in (8) accounts for the case of small localization length $\xi \ll 1$ when $r_l \ll 1$ but the volume is approximately one lattice site. We plot the value of r_l as a function of θ in the inset of Fig. 4. The proportionality factor f can be assumed to be of order one. To get a number, we use the data for $\theta = 0.45\pi$ in Fig. 2 to read off $V_{\rm loc} \approx 70$ and arrive at the value $f \approx 2$ which we will use for all other curve analysis as well. The outcome is shown by the blue (top) curve in Fig. 4. We find that $T_f(\theta)$ is expected to have a minimum at around $\theta = 0.45\pi$, while it is growing substantially when deviating to larger and smaller values of θ.

Derivation. In order to explain the observed logarithmic expansion and the subsequent halt, we assume that the localization length $\xi \gg 1$ and thus $r_l \gg 1$. In order to enter the logarithmic expansion regime with $r(t) > r_l$, the wave-packet

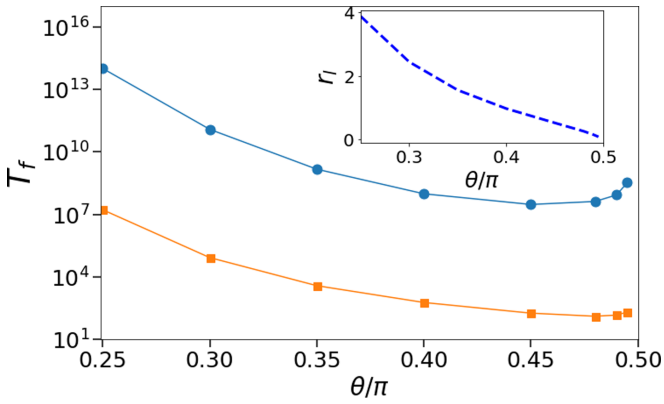

FIG. 4. T_f vs θ. Blue top curve data are extracted from the data in Fig. 2 following Eq. (7). For the fit details, see the text. Orange bottom curve—result of theoretical analysis. Inset: The saturated rms r_l for a single particle as a function of θ.

density must be small such that at any given time for most of the wave-packet sites the quantization condition (5) yields one particle, i.e., $\lfloor N\rho \rfloor = 0$. For a large time the dynamics in a localization volume v_l will be following the linear DTQW dynamics. We assume (and tested numerically) that the local norm on any of the two levels in a two-level system will fluctuate following an exponential (Gibbs) distribution $\sim e^{-\mu\rho}$ with chemical potential $\mu = 2r$ (inverse of average local norm). The fluctuations are restricted to norm redistributions within the finite volume $v_l \approx r_l$ and have an upper limit $\rho_{\max} = cr_l/r(t) > 1/N$ with the constant c being of order one and to be fixed below. Then the norm ρ_n on the entire two-level system will fluctuate according to the distribution of the sum of two uncorrelated non-negative random numbers

$$\mathcal{P}(\rho_n) = \mu^2 \rho_n e^{-\mu\rho_n}, \quad 0 \leqslant \rho_n \leqslant \rho_{\max}. \tag{9}$$

There is a small but finite probability $\wp$ that $1/N < \rho_n < \rho_{\max}$:

$$\wp(r) = \int_{1/N}^{\rho_{\max}} \mathcal{P} d\rho_n \approx e^{-2r/N} - e^{-2cr_l}. \tag{10}$$

The average time for that to happen is $T \approx 1/\wp$. Once the rare event takes place, the quantized nonlinearity (5) effectively changes the disorder potential within the considered localization volume. At the edge of the wave packet, that leads to an expansion into a newly accessible localization volume:

$$\frac{dr}{dt} = r_l \wp(r), \quad r(t) = Ncr_l + \frac{N}{2} \ln\left(1 - e^{-\frac{2r_l t}{Ne^{2cr_l}}}\right). \tag{11}$$

It follows that $r(t \to \infty) \to Ncr_l$ and with (8) we conclude $c \approx f$. We are now in a position to obtain the logarithmic expansion law, which is derived from (11):

$$r(t) = \frac{N}{2} \ln\left(\frac{2r_l}{N}\right) + \frac{N}{2} \ln(t), \quad t \ll \frac{Ne^{2fr_l}}{2r_l}. \tag{12}$$

The fitting parameter r_0 from Eq. (6) corresponds to the first term on the right-hand side (rhs) of (12). The logarithmic expansion is universal in the sense that the slope $N/2$ depends only on the particle number, but not on the particularities of the disorder, nonlinearity, and ramping. In our numerical computations in Fig. 3 we used $N = 24$. The observed slope $\approx$20 was measured on logarithmic timescales in base 10 and matches reasonably well with the theoretical prediction $\frac{N}{2} \ln 10 = 27.6$. Finally we can attempt to estimate the saturation time T_f from (11). For that we compute the time at which the exponent in the rhs in (11) is of order one. The result reads

$$T_f = \frac{Ne^{2fr_l}}{2r_l}. \tag{13}$$

It follows that the saturation time diverges exponentially with large r_l in the limit of infinite localization length $\theta \to 0$. At the same time the saturation time diverges as $1/r_l$ in the limit of small localization length $\theta \to \pi/2$. Therefore there must be a minimum saturation time T_f at some value of θ. The full dependence of $T_f(\theta)$ is plotted in Fig. 4. We find that the minimum saturation time is obtained for $\theta \approx 0.48\pi$ which is reasonably close to the numerically observed value $\approx 0.45\pi$. Note that the absolute values of the theoretical estimate of T_f are much lower than the computational results. The reason is that our theoretical approach is qualitative when it comes to fitting, and operates on logarithmic scales. Changing V_{loc} from 70 to around 80 changes f from 2 to 2.3. An additional replacement of r_l by $r_l + 1$ results in a magnitude shift of T_f upwards by three orders of magnitude. Despite the qualitative character of the theory, it is capable of reproducing the universal log law, and the minimum in T_f.

Discussion. The wave packet starts to spread in a ballistic-like regime up to the size of the single-particle localization volume v_l. It then enters a subdiffusive regime when not ramped, or diffusive regime when ramped which extends until the start of the logarithmic regime due to density quantization which happens for a wave-packet size of the order of N and at a time $t \sim N^2/D$. The spreading finally halts for a packet size of the order of Nv_l. Therefore both the logarithmic part and the halt are scaled to infinite times in the limit $N \to \infty$, which recovers a familiar (sub)diffusion of the wave packet on all accessible timescales known for the nonquantized theory [35]. If instead the single-particle localization volume v_l is tuned to larger and larger values, the logarithmic spreading part is extending over more and more time decades. The crossover between the (sub)diffusion and the logarithmic regimes is scaled to shorter times. This follows from the dependence of the diffusion constant D on the localization length [33]. The (sub)diffusive regime window is closing completely for $v_l > N$ so that the ballistic regime is immediately followed by the logarithmic one. All these results can be read off the data in Fig. 2.

Experimental platforms which use ultracold atomic gases [25] can keep cloud coherence up to times which are comparable to 10^4 of our dimensionless time units [33]. Interaction strength ramping using Feshbach resonances is feasible. Therefore we conclude that such experimental platforms can observe the onset of logarithmic spreading (see the curve for $\theta = 0.25\pi$ in Fig. 3).

Conclusion. Nonlinear wave packets spread subdiffusively in a disordered environment. Despite many efforts to observe a slowing down of the subdiffusion, all computational evidence points to unlimited subdiffusion. Quantum systems with many particles and a conserved particle number were expected to be sufficient for a slowing down from subdiffusion and final halt of spreading for finite particle numbers. In this Letter we simulate this effect using a rough action quantization of a nonlinear wave propagation. To actually reach the desired timescales, we chose highly efficient unitary maps (discrete-time quantum walks) and nonlinear interaction strength ramping for computational speedup. We succeeded with observing the halt of expansion. In addition, we discovered an intermediate logarithmic expansion regime whose time window grows with increasing localization length. In that regime the speed of the wave-packet size growth on logarithmic timescales depends only on the total particle number in the packet.

Acknowledgments. We thank M. Malishava and I. Vakulchyk for helpful discussions. This work was supported by the Institute for Basic Science in Korea (IBS-R024-D1).

[1] P. W. Anderson, Absence of diffusion in certain random lattices, Phys. Rev. **109**, 1492 (1958).

[2] I. M. Lifshitz, S. A. Gredeskul, and L. A. Pastur, *Introduction to the Theory of Disordered Systems* (Wiley, New York 1988).

[3] B. Kramer and A. MacKinnon, Localization: theory and experiment, Rep. Prog. Phys. **56**, 1469 (1993).

[4] J. Billy, V. Josse, Z. Zuo, A. Bernard, B. Hambrecht, P. Lugan, D. Clément, L. Sanchez-Palencia, P. Bouyer, and A. Aspect, Direct observation of Anderson localization of matter waves in a controlled disorder, Nature (London) **453**, 891 (2008).

[5] D. L. Shepelyansky, Coherent Propagation of Two Interacting Particles in a Random Potential, Phys. Rev. Lett. **73**, 2607 (1994).

[6] Y Imry, Coherent propagation of two interacting particles in a random potential, Europhys. Lett. **30**, 405 (1995).

[7] K. Frahm, A. Müller-Groeling, J.-L Pichard, and D. Weinmann, Scaling in interaction-assisted coherent transport, Europhys. Lett. **31**, 169 (1995).

[8] F. von Oppen, T. Wettig, and J. Müller, Interaction-Induced Delocalization of Two Particles in a Random Potential: Scaling Properties, Phys. Rev. Lett. **76**, 491 (1996).

[9] Ph. Jacquod, D. L. Shepelyansky, and O. P. Sushkov, Breit-Wigner Width for Two Interacting Particles in a One-Dimensional Random Potential, Phys. Rev. Lett. **78**, 923 (1997).

[10] R. A. Römer and M. Schreiber, No Enhancement of the Localization Length for Two Interacting Particles in a Random Potential, Phys. Rev. Lett. **78**, 515 (1997).

[11] I. V. Ponomarev and P. G. Silvestrov, Coherent propagation of interacting particles in a random potential: The mechanism of enhancement, Phys. Rev. B **56**, 3742 (1997).

[12] P. H. Song and D. Kim, Localization of two interacting particles in a one-dimensional random potential, Phys. Rev. B **56**, 12217 (1997).

[13] R. A. Römer, M. Schreiber, and T. Vojta, Two interacting particles in a random potential: Numerical calculations of the interaction matrix elements, Phys. Status Solidi B **211**, 681 (1999).

[14] K. M. Frahm, Interaction induced delocalization of two particles: large system size calculations and dependence on interaction strength, Eur. Phys. J. B **10**, 371 (1999).

[15] P. H. Song and F. von Oppen, General localization lengths for two interacting particles in a disordered chain, Phys. Rev. B **59**, 46 (1999).

[16] S. De Toro Arias, X. Waintal, and J.-L. Pichard, Two interacting particles in a disordered chain III: Dynamical aspects of the interplay disorder-interaction, Eur. Phys. J. B **10**, 149 (1999).

[17] D. O. Krimer, R. Khomeriki, and S. Flach, Two interacting particles in a random potential, JETP Lett. **94**, 406 (2011).

[18] M. V. Ivanchenko, T. V. Laptyeva, and S. Flach, Quantum chaotic subdiffusion in random potentials, Phys. Rev. B **89**, 060301(R) (2014).

[19] D. O. Krimer and S. Flach, Interaction-induced connectivity of disordered two-particle states, Phys. Rev. B **91**, 100201(R) (2015).

[20] K. M. Frahm, Eigenfunction structure and scaling of two interacting particles in the one-dimensional Anderson model, Eur. Phys. J. B **89**, 115 (2016).

[21] I. I. Yusipov, T. V. Laptyeva, A. Yu. Pirova, I. B. Meyerov, S. Flach, and M. V. Ivanchenko, Quantum subdiffusion with two- and three-body interactions, Eur. Phys. J. B **90**, 1 (2017).

[22] D. Thongjaomayum, A. Andreanov, T. Engl, and S. Flach, Taming two interacting particles with disorder, Phys. Rev. B **100**, 224203 (2019).

[23] M. Malishava, I. Vakulchyk, M. Fistul, and S. Flach, Floquet Anderson localization of two interacting discrete time quantum walks, Phys. Rev. B **101**, 144201 (2020).

[24] G. Schwiete and A. M. Finkel'stein, Kinetics of the disordered Bose gas with collisions, Phys. Rev. A **88**, 053611 (2013).

[25] E. Lucioni, B. Deissler, L. Tanzi, G. Roati, M. Zaccanti, M. Modugno, M. Larcher, F. Dalfovo, M. Inguscio, and G. Modugno, Observation of Subdiffusion in a Disordered Interacting System, Phys. Rev. Lett. **106**, 230403 (2011).

[26] D. L. Shepelyansky, Delocalization of Quantum Chaos by Weak Nonlinearity, Phys. Rev. Lett. **70**, 1787 (1993).

[27] A. S. Pikovsky and D. L. Shepelyansky, Destruction of Anderson Localization by a Weak Nonlinearity, Phys. Rev. Lett. **100**, 094101 (2008).

[28] S. Flach, D. O. Krimer, and Ch. Skokos, Universal Spreading of Wave Packets in Disordered Nonlinear Systems, Phys. Rev. Lett. **102**, 024101 (2009) [Erratum: **102**, 209903 (2009)].

[29] T. V. Laptyeva, J. D. Bodyfelt, D. O. Krimer, Ch. Skokos, and S. Flach, The crossover from strong to weak chaos for nonlinear waves in disordered systems, Europhys. Lett. **91**, 30001 (2010).

[30] M. V. Ivanchenko, T. V. Laptyeva, and S. Flach, Anderson Localization or Nonlinear Waves: A Matter of Probability, Phys. Rev. Lett. **107**, 240602 (2011).

[31] Y. Kati, X. Yu, and S. Flach, Density resolved wave packet spreading in disordered Gross-Pitaevskii lattices, SciPost Phys. Core **3**, 006 (2020).

[32] L. Ermann and D. L. Shepelyansky, Deconfinement of classical Yang–Mills color fields in a disorder potential, Chaos **31**, 093106 (2021).

[33] T. V. Laptyeva, M. V. Ivanchenko, and S. Flach, Nonlinear lattice waves in heterogeneous media, J. Phys. A: Math. Theor. **47**, 493001 (2014).

[34] I. Vakulchyk, M. V. Fistul, P. Qin, and S. Flach, Anderson localization in generalized discrete-time quantum walks, Phys. Rev. B **96**, 144204 (2017).

[35] I. Vakulchyk, M. V. Fistul, and S. Flach, Wave Packet Spreading with Disordered Nonlinear Discrete-Time Quantum Walks, Phys. Rev. Lett. **122**, 040501 (2019).

[36] G. Gligorić, K. Rayanov, and S. Flach, Make slow fast—how to speed up interacting disordered matter, Europhys. Lett. **101**, 10011 (2013).

[37] B. V. Chirikov, F. M. Izrailev, and D. L. Shepelyansky, Dynamical stochasticity in classical and quantum mechanics, Sov. Sci. Rev., Sect. C **2**, 209 (1981).

[38] G. P. Berman, A. R. Kolovsky, and F. M. Izrailev, Quantum chaos and peculiarities of diffusion in wigner representation, Physica A **152**, 273 (1988).

[39] G. P. Berman, A. R. Kolovskĭ, F. M. Izrailev, and A. M. Iomin, Quantum chaos in the Wigner representation, Chaos **1**, 220 (1991).

[40] I. Guarneri, G. Casati, and V. Karle, Classical Dynamical Localization, Phys. Rev. Lett. **113**, 174101 (2014).

[41] Y. Aharonov, L. Davidovich, and N. Zagury, Quantum random walks, Phys. Rev. A **48**, 1687 (1993).

[42] D. A. Meyer, From quantum cellular automata to quantum lattice gases, J. Stat. Phys. **85**, 551 (1996).

[43] A. Mallick, and C. M. Chandrashekar, Dirac cellular automaton from split-step quantum walk, Sci. Rep. **6**, 25779 (2016).

[44] A. Mallick, Quantum simulation of neutrino oscillation and Dirac particle dynamics in curved space-time, Ph.D. thesis, Homi Bhabha National Institute, 2018, arXiv:1901.04014.

[45] P. Arnault and F. Debbasch, Quantum walks and discrete gauge theories, Phys. Rev. A **93**, 052301 (2016).

[46] T. Kitagawa, M. S. Rudner, E. Berg, and E. Demler, Exploring topological phases with quantum walks, Phys. Rev. A **82**, 033429 (2010).

[47] J. K. Asbóth, Symmetries, topological phases, and bound states in the one-dimensional quantum walk, Phys. Rev. B **86**, 195414 (2012).

[48] J. K. Asbóth and A. Mallick, Topological delocalization in the completely disordered two-dimensional quantum walk, Phys. Rev. B **102**, 224202 (2020).

[49] C. M. Chandrashekar and Th. Busch, Quantum percolation and transition point of a directed discrete-time quantum walk, Sci. Rep. **4**, 6583 (2014).

[50] B. Kollár, J. Novotný, T. Kiss, and I. Jex, Discrete time quantum walks on percolation graphs, Eur. Phys. J. Plus **129**, 103 (2014).

[51] B. Kollár, A. Gilyén, I. Tkáčová, T. Kiss, I. Jex, and M. Štefaňák, Complete classification of trapping coins for quantum walks on the two-dimensional square lattice, Phys. Rev. A **102**, 012207 (2020).

[52] P. Chawla, R. Mangal, and C. M. Chandrashekar, Discrete-time quantum walk algorithm for ranking nodes on a network, Quantum Inf. Process. **19**, 158 (2020).

[53] S. Srikara and C. M. Chandrashekar, Quantum direct communication protocols using discrete-time quantum walk, Quantum Inf. Process. **19**, 295 (2020).

[54] C. Vlachou, W. Krawec, P. Mateus, N. Paunković, and A. Souto, Quantum key distribution with quantum walks, Quantum Inf. Process. **17**, 288 (2018).

[55] C. A. Ryan, M. Laforest, J. C. Boileau, and R. Laflamme, Experimental implementation of a discrete-time quantum random walk on an NMR quantum-information processor, Phys. Rev. A **72**, 062317 (2005).

[56] A. Crespi, R. Osellame, R. Ramponi, V. Giovannetti, R. Fazio, L. Sansoni, F. De Nicola, F. Sciarrino, and P. Mataloni, Anderson localization of entangled photons in an integrated quantum walk, Nat. Photonics **7**, 322 (2013).

[57] Q.-P. Su, Y. Zhang, L. Yu, J.-Q. Zhou, J.-S. Jin, X.-Q. Xu, S.-J. Xiong, Q. Xu, Z. Sun, K. Chen *et al.*, Experimental demonstration of quantum walks with initial superposition states, npj Quantum Inf. **5**, 40 (2019).

[58] F. Acasiete, F. P. Agostini, J. K. Moqadam, and R. Portugal, Implementation of quantum walks on IBM quantum computers, Quantum Inf. Process. **19**, 426 (2020).

[59] C. Huerta Alderete, S. Singh, N. H. Nguyen, D. Zhu, Radhakrishnan Balu, Christopher Monroe, C. M. Chandrashekar, and N. M. Linke, Quantum walks and Dirac cellular automata on a programmable trapped-ion quantum computer, Nat. Commun. **11**, 3720 (2020).

[60] C. Navarrete-Benlloch, A. Pérez, and E. Roldán, Nonlinear optical Galton board, Phys. Rev. A **75**, 062333 (2007).

[61] M. Maeda, H. Sasaki, E. Segawa, A. Suzuki, and K. Suzuki, Dynamics of solitons for nonlinear quantum walks, J. Phys. Commun. **3**, 075002 (2019).

[62] M. Maeda and A. Suzuki, Continuous limits of linear and nonlinear quantum walks, Rev. Math. Phys. **32**, 2050008 (2020).

[63] K. Mochizuki, N. Kawakami, and H. Obuse, Stability of topologically protected edge states in nonlinear quantum walks: additional bifurcations unique to Floquet systems, J. Phys. A: Math. Theor. **53**, 085702 (2020).

[64] R. Adami, R. Fukuizumi, and E. Segawa, A nonlinear quantum walk induced by a quantum graph with nonlinear delta potentials, Quantum Inf. Process. **18**, 119 (2019).

[65] S. Flach, Spreading of waves in nonlinear disordered media, Chem. Phys. **375**, 548 (2010).

[66] S. Inouye, M. R. Andrews, J. Stenger, H.-J. Miesner, D. M. Stamper-Kurn, and W. Ketterle, Observation of Feshbach resonances in a Bose–Einstein condensate, Nature (London) **392**, 151 (1998).

[67] L. Khaykovich, F. Schreck, G. Ferrari, T. Bourdel, J. Cubizolles, L. D. Carr, Y. Castin, and C. Salomon, Formation of a matter-wave bright soliton, Science **296**, 1290 (2002).

[68] T. Weber, J. Herbig, M. Mark, H.-C. Nägerl, and R. Grimm, Bose-Einstein condensation of cesium, Science **299**, 232 (2003).

[69] G. Roati, M. Zaccanti, C. D'Errico, J. Catani, M. Modugno, A. Simoni, M. Inguscio, and G. Modugno, ^{39}K Bose-Einstein Condensate with Tunable Interactions, Phys. Rev. Lett. **99**, 010403 (2007).

[70] F. Dalfovo, S. Giorgini, L. P. Pitaevskii, and S. Stringari, Theory of Bose-Einstein condensation in trapped gases, Rev. Mod. Phys. **71**, 463 (1999).

[71] A. Smerzi and A. Trombettoni, Nonlinear tight-binding approximation for Bose-Einstein condensates in a lattice, Phys. Rev. A **68**, 023613 (2003).